Title:

A Type VI Secretion System in *Burkholderia* Species *cenocepacia* and *orbicola* Triggers Distinct Macrophage Death Pathways Independent of the Pyrin Inflammasome

Authors:

Nicole A. Loeven[1,2], Arianna D. Reuven[1], Abigail P. McGee[1], Clarrisa Dabi[1], Bethany W. Mwaura[1] and James B. Bliska[1,3]

[1]Department of Microbiology and Immunology, Geisel School of Medicine at Dartmouth College, Hanover, NH, USA

[2]Current address: Department of Pathology and Laboratory Medicine, Hospital of the University of Pennsylvania, Philadelphia, Pennsylvania, USA

[3]Correspondiing author: james.bliska@dartmouth.edu

Abstract

The *Burkholderia cepacia* complex contains opportunistic pathogens that cause chronic infections and inflammation in lungs of people with cystic fibrosis. Two closely related species within this complex are *Burkholderia cenocepacia* and the recently classified *Burkholderia orbicola*. *B. cenocepacia* and *B. orbicola* encode a type VI secretion system and the effector TecA, which is detected by the pyrin/caspase-1 inflammasome, and triggers macrophage inflammatory death. In our earlier study the pyrin inflammasome was dispensable for lung inflammation in mice infected with *B. orbicola* AU1054, indicating this species activates an alternative pathway of macrophage inflammatory death. Notably, *B. cenocepacia* J2315 and K56-2 can damage macrophage phagosomes and K56-2 triggers activation of the caspase-11 inflammasome, which detects cytosolic LPS. Here we investigated inflammatory cell death in pyrin-deficient (*Mefv*$^{-/-}$) mouse macrophages infected with *B. cenocepacia* J2315 or K56-2 or *B. orbicola* AU1054 or PC184. Macrophage inflammatory death was measured by cleavage of gasdermin D protein, release of cytokines IL-1α and IL-1β and plasma membrane rupture. Findings suggest that J2315 and K56-2 are detected by the caspase-11 inflammasome in *Mefv*$^{-/-}$ macrophages, resulting in IL-1β release. In contrast, inflammasome activation is not detected in *Mefv*$^{-/-}$ macrophages infected with AU1054 or PC184. Instead, AU1054 triggers an alternative macrophage inflammatory death pathway that requires TecA and results in plasma membrane rupture and IL-1α release. Amino acid variation between TecA isoforms in *B. cenocepacia* and *B. orbicola* may explain how the latter species triggers a non-inflammasome macrophage death pathway.

41 **Introduction**

42 The *Burkholderia cepacia* complex (Bcc) comprise a group of Gram-negative bacterial species
43 that exist in the environment (1). The Bcc are opportunistic pathogens that cause infections in
44 immunocompromised individuals including people with cystic fibrosis (pwCF) (1). The Bcc
45 typically cause chronic infections associated with inflammation and exacerbations in adult
46 pwCF. Chronic infections are difficult to eliminate due to intrinsic antibiotic resistance in the Bcc.
47 Chronic Bcc infections can progress to an acute disease called cepacia syndrome that is
48 characterized by necrotizing pneumonia, bacteremia, and sepsis. *B. cenocepacia* accounts for
49 ~45% of Bcc isolates from pwCF in the United States and is considered one of the most virulent
50 in this group because of its strong association with cepacia syndrome (2, 3). In addition, *B.*
51 *cenocepacia* infection is a contraindication for lung transplantation (4). *B. cenocepacia*
52 subgrouping based on *recA* lineages has resulted in classification of genomovars IIIA-D (5) and
53 shown that isolates belonging to genomovar IIIA commonly circulate in the UK, Europe, and
54 Canada, while genomovar IIIB isolates more commonly cause infections in pwCF in the United
55 States (6).
56
57 *B. cenocepacia* encodes numerous virulence factors (1, 7) and preferentially resides within
58 phagocytes in the CF lung (8-10). Residence of *B. cenocepacia* in phagocytes has been
59 observed by in situ imaging of human lung sections from transplant or autopsy, or mouse lung
60 sections from experimental infections (11, 12). *B. cenocepacia* resides in vacuoles in phagocytic
61 cells (11, 12), but may damage phagosomes and escape into the cytosol as well (13, 14).
62 Additionally, *B. cenocepacia* can invade and survive in airway epithelial cells which may play a
63 role in transmigration across the epithelial barrier (7). The intracellular location of *B.*
64 *cenocepacia* appears to be key to its pathogenesis (8). *B. cenocepacia* can prevent
65 phagosomal maturation and delay co-localization of the NADPH oxidase complex with the
66 vacuolar membrane (15, 16). CF macrophages display defects in oxidative burst (17) and

67 bacteria-specific autophagy (xenophagy) (9, 10) which may render them permissive to *B.*
68 *cenocepacia.* In non-CF macrophages, phagosome damage by *B. cenocepacia* increases
69 xenophagy (18) but the pathogen may be able to subvert this bactericidal process for
70 intracellular survival (13). In addition, type I interferon production by non-CF macrophages in
71 response to cytosolic *B. cenocepacia* infection can act in an autocrine fashion to increase
72 xenophagy and limit bacterial replication (14).
73
74 A *B. cenocepacia* virulence factor implicated in lung infection and intracellular pathogenesis a
75 type VI secretion system (T6SS) (8, 19). The T6SS contains a tube-like structure that functions
76 to deliver effectors into bacteria or host cells (20, 21). Upon contact with target cells the tube
77 comprised of the Hcp protein fires to puncture membranes and release associated effectors.
78 The effectors have enzymatic activity that modify and inactivate key cellular processes or
79 structures in target cells. The *B. cenocepacia* T6SS belongs to the first of three classes of these
80 systems to be characterized ($T6SS^{i}$, $T6SS^{ii}$ and $T6SS^{iii}$) (21). The $T6SS^{i}$ class is common
81 within Gammaproteobacteria and since the *B. cenocepacia* system is homologous to T6SS-1 of
82 *Burkholderia pseudomallei* (22) we hereafter referred to it as T6SS-1. T6SS-1 is required for
83 intracellular *B. cenocepacia* to inactivate small GTPases including Rac1 and Cdc42, resulting in
84 disruption of the actin cytoskeleton and preventing assembly of the NADPH oxidase complex in
85 macrophages (23, 24).
86
87 T6SS-1 is detected by inflammasomes in macrophages harboring *B. cenocepacia* (18, 25-27).
88 Canonical caspase-1 inflammasomes are assembled when sensors such as NLRP3, NLRC4 or
89 pyrin detect danger signals generated by bacterial pathogens during infection of host cells (28).
90 Active caspase-1 is produced and cleaves the pro-inflammatory cytokine pro-IL-1β and the
91 gasdermin-D (GSDMD) protein (29). Cleavage of GSDMD releases a domain that oligomerizes
92 and forms pores in the plasma membrane (29). Mature IL-1β leaks out of these pores and can

93 stimulate inflammatory signaling through activation of the IL-1 receptor found on a variety of
94 host cells (29). Pore formation in plasma membranes can also result in pyroptosis, a pro-
95 inflammatory form of cell death (29).
96
97 Early studies implicated T6SS-1 of *B. cenocepacia* strain K56-2 (genomovar IIIA, Table 1) in
98 activation of the NLRP3 and NLRC4 inflammasomes in murine macrophages and the pyrin
99 inflammasome in human macrophages (25, 26). Assembly of the pyrin inflammasome in
100 response to T6SS-1 was subsequently observed in murine macrophages infected with J2315
101 (genomovar IIIA, Table 1) (27). Pyrin inflammasome assembly in macrophages infected with
102 J2315 required inactivation of RhoA by T6SS-1 (27). The T6SS-1 in K56-2 has also been
103 shown to be detected by the non-canonical caspase-11 inflammasome in murine macrophages
104 (18, 30), which is consistent with phagosome damage (26) and entry of LPS into the cytosol
105 (31). Caspase-11 can cleave GSDMD to form pores in macrophages but requires activation of a
106 caspase-1 inflammasome (e.g. NLRP3) for processing and release of IL-1β (31).
107
108 Aubert et al. identified TecA (T6SS effector protein affecting cytoskeletal architecture) as being
109 responsible for inactivation of RhoA and assembly of the pyrin inflammasome in macrophages
110 infected with K56-2 or J2315 (32). In silico modeling of *B. cenocepacia* TecA predicted a fold
111 consistent with a cysteine protease-like hydrolase, and putative catalytic C41, H105 and D149
112 residues were confirmed by mutagenesis (32). TecA appears to be the founding member of a
113 T6SS effector superfamily with deamidase activity in bacterial opportunistic pathogens and
114 symbionts (32). After entry into phagocytes *B. cenocepacia* employs the T6SS-1 to deliver TecA
115 across the phagosome into the cytosol (32). RhoA is inactivated in response to deamidation of
116 Asn-41 by TecA (32). Assembly of the pyrin inflammasome in response to deamidation of RhoA
117 by TecA in macrophages infected with *B. cenocepacia* is an example of a guard mechanism of
118 effector-triggered immunity (32). More recently TecA has been shown to promote localized

119 actin polymerization that delays maturation of phagosomes containing J2315 in macrophages
120 (33).
121
122 Previous studies examined the role of pyrin and TecA in lung pathogenesis by intranasally
123 infecting C57BL/6 mice with J2315 (27, 32). Xu et al. compared C57BL/6 and pyrin knockout
124 (*Mefv*$^{-/-}$) mice and found that J2315 infection stimulated inflammatory cell infiltration into lungs of
125 C57BL/6 but not *Mefv*$^{-/-}$ mice (27). Aubert et al. infected C57BL/6 mice with J2315 or a Δ*tecA*
126 mutant and reported that TecA was important for inflammatory cell infiltration and acute lung
127 damage (32).
128
129 Increasing numbers of whole genome sequences for *Burkholderia* strains are being determined
130 and analyzed. Results of two recent genomic analysis studies have suggested that genomovar
131 IIIB isolates be designated as a species separate from *B. cenocepacia* (34, 35). Morales-Ruíz et
132 al. propose for the new species the name *B. orbicola* (35). This name comes from the Latin
133 word *orbis* and suffix -*cola* meaning "the whole world" and "dweller" respectively, making
134 *orbicola* "inhabitant of the whole world" (35). Here, we follow this convention and hereafter refer
135 to genomovar IIIB strains as *B. orbicola*.
136
137 *B. orbicola* strain AU1054 (Table 1), isolated from the bloodstream of a CF patient, encodes
138 T6SS-1 (36) and TecA (37). Results of murine macrophage infections in vitro showed that
139 AU1054 TecA triggers release of IL-1β in a T6SS-1- and pyrin-dependent manner (37). In an
140 infection model using C57BL/6 or CF mice (mice with the most common CFTR mutation in
141 humans, F508del) with AU1054 we confirmed that TecA is important for inflammatory cell
142 recruitment to lungs (37). Surprisingly, using *Mefv*$^{-/-}$ mice in the CF or non-CF background we
143 were unable to reproduce a role for pyrin in inflammatory cell accumulation in lungs during

144 infection with AU1054 or J2315 (37). This finding led us to hypothesize that AU1054 and J2315
145 can trigger inflammation by a mechanism independent of the pyrin inflammasome. Notably,
146 J2315 been shown to damage macrophage phagosomes (13), which would allow detection by
147 the non-canonical inflammasome, similar to its clonal relative K56-2 (18, 30). Activation of the
148 caspase-11 inflammasome has been shown to contribute to lung inflammation and
149 immunopathology in mice infected with K56-2 (18).
150
151 Here we investigated pyrin-independent macrophage inflammatory cell death in response to
152 infection with *B. cenocepacia* J2315 or *B. orbicola* AU1054. Results indicate that J2315 and
153 AU1054 trigger distinct pyrin-independent macrophage inflammatory death pathways with
154 different inflammasome and TecA requirements. Amino acid differences between TecA protein
155 sequences of *B. cenocepacia* and *B. orbicola* strains were identified, suggesting distinct effector
156 isoform activities. These data have important implications for understanding the role of T6SS-1
157 and TecA in macrophage inflammatory death and the pathogenesis of chronic lung infections
158 caused by *B. cenocepacia* and *B. orbicola* in pwCF.
159
160 **Results**
161
162 **Pyrin is differentially required for gasdermin-D cleavage in macrophages infected with *B.***
163 ***cenocepacia* or *B. orbicola*.** To determine if AU1054 and J2315 can trigger inflammasome
164 activation independent of pyrin, bone marrow derived macrophages (BMDMs) from *Mefv*$^{+/+}$ or
165 *Mefv*$^{-/-}$ C57BL/6 mice were LPS primed, infected for 90 min and cleavage of GSDMD was
166 measured by immunoblotting. For control strains we used AU1054 Δ*tecA* and Δ*hcp* mutants which
167 are unable to trigger the pyrin inflammasome (37) and K56-2 which activates the caspase-11
168 inflammasome (18, 30) (Table 1). As expected GSDMD cleavage in BMDMs infected with
169 AU1054 required TecA, Hcp and pyrin (Fig.1, lanes 2-4, 8-10). Interestingly, GSDMD was
170 cleaved in *Mefv*$^{+/+}$ and *Mefv*$^{-/-}$ BMDMs infected with J2315 (isolate A, Table 1), like K56-2 (Fig.1,

171 lanes 5,6 and 11,12). These results suggest that J2315 can, like K56-2, activate a pyrin-
172 independent inflammasome in macrophages.
173
174 To determine if the phenotype we observed was specific to the J2315 A isolate from our
175 laboratory, several additional isolates obtained from other investigators (Isolates B-D, Table 1)
176 were analyzed in infections with *Mefv*$^{+/+}$ and *Mefv*$^{-/-}$ BMDMs. GSDMD was cleaved in *Mefv*$^{-/-}$
177 BMDMs infected with all isolates (Fig.2A, lanes 8,9 and Fig.2B, lanes 7-9), indicating that pyrin-
178 independent inflammasome activation and GSDMD cleavage is a general property of J2315.
179
180 We also infected *Mefv*$^{+/+}$ and *Mefv*$^{-/-}$ BMDMs with an additional *B. orbicola* isolate, PC184 (Table
181 1), and found that pyrin was required for cleavage of GSDMD (Fig.2B, lanes 5,10), like AU1054.
182 These results suggest that *B. orbicola* and *B. cenocepacia* differ in the ability to activate
183 inflammasomes in macrophages independent of pyrin.
184
185 **TecA is dispensable for pyrin-independent GSDMD cleavage and IL-1β release in**
186 **macrophages infected with J2315.** To determine if TecA is required for J2315 to trigger pyrin-
187 independent GSDMD cleavage and IL-1β release, we obtained an additional isolate (Isolate E)
188 of this strain and its corresponding Δ*tecA* mutant (32) (Table 1). LPS-primed *Mefv*$^{+/+}$ or *Mefv*$^{-/-}$
189 BMDMs infected with these strains or AU1054 controls were analyzed for GSDMD cleavage as
190 well as IL-1β release. As expected from our previous ELISA results (37) and the GSDMD
191 cleavage data presented here (Figs.1, 3A), TecA and pyrin were required for significant release
192 of IL-1β from BMDMs infected with AU1054 (Fig.3B). However, findings here showed that TecA
193 and pyrin were not required for GSDMD cleavage (Fig.3A, lane 11) or IL-1β release BMDMs
194 infected with J2315 (Fig.3C). Additional experiments are needed to solidify these findings
195 because the IL-1β values for the J2315 samples showed variability. Nevertheless, these results

196 are consistent with the idea that J2315, like K56-2, can activate both pyrin and the caspase-11
197 inflammasomes in macrophages (18). This conclusion will need to be verified using *Casp11*$^{-/-}$
198 BMDMs in future experiments.
199
200 **TecA triggers pyrin inflammasome-independent IL-1α and LDH release from macrophages**
201 **infected with AU1054.** To determine if AU1054 triggers another form of pyrin-independent
202 macrophage inflammatory death, we measured release of IL-1α and LDH. IL-1α can be released
203 from macrophages by inflammasome-dependent and -independent mechanisms. In the latter
204 case plasma-membrane rupture (PMR) allows IL-1α to be released from host cells to act as a
205 danger-associated-molecular pattern (DAMP) (38). LDH at 140 kDa is a marker of PMR. These
206 experiments used *Mefv*$^{+/+}$ or *Mefv*$^{-/-}$ BMDMs from mice engineered with a CF genotype (*Cftr*^{F508del})
207 and after LPS priming they were left uninfected or infected with AU1054 or AU1054 Δ*tecA* as
208 above. For a positive control we treated the BMDMs with *Clostridium difficile* TcdB toxin and the
209 culture supernatants were analyzed by ELISA for IL-1β, which is dependent upon inflammasome
210 activation for processing and release. As shown in Fig.4A, significant IL-1β release upon AU1054
211 infection required TecA and pyrin as expected. However, pyrin was not required for TecA to
212 trigger release of IL-1α (Fig.4B) or LDH (Fig.4C) from *Mefv*$^{-/-}$ BMDMs infected with AU1054. IL-
213 1α released in response to AU1054 infection was significantly lower in *Mefv*$^{-/-}$ as compared to
214 *Mefv*$^{+/+}$ or BMDMs (Fig.4B), likely because pyrin inflammasome activation contributed to secretion
215 of the cytokine in the former case. IL-1α and LDH released from *Mefv*$^{-/-}$ BMDMs intoxicated with
216 TcdB was at background levels (Fig.4B, C respectively). These data suggest that AU1054 TecA
217 triggers an inflammasome-independent mechanism of PMR leading to macrophage inflammatory
218 death.
219

220 **The TecA proteins of *B. orbicola* and *B. cenocepacia* exhibit amino acid variation.** The
221 ability of AU1054 TecA to trigger inflammasome-independent PMR in BMDMs (Fig.4) suggested
222 that the *orbicola* isoform has distinct biological function/activity as compared to the canonical
223 *cenocepacia* effector. To examine this possibility, we sequenced *tecA* genes from isolates used
224 in this study. The resulting predicted TecA protein sequences were aligned using ClustalW
225 (Fig.5). The *B. cenocepacia* J2315 and K56-2 proteins are 100% identical and the *B. orbicola*
226 AU1054 and PC184 proteins are 99% identical (Fig.5). In contrast, *B. cenocepacia* TecA
227 shares only ~90% sequence identity with the *B. orbicola* isoform, due to 15-16 amino acid
228 differences (Fig.5).
229
230 All TecA isoforms have residues C41, H105 and D148 that are important for catalytic activity
231 (32, 37) (Fig.5). In addition, amino acids immediately flanking the catalytic residues are highly
232 conserved between *B. cenocepacia* and *B. orbicola* (Fig.5). However, *B. orbicola* TecA has
233 non-conserved substitutions R38G (charged to non-charged), G101T (non-polar to polar), and
234 T146A (polar to non-polar) within 3, 4 and 2 amino acids of C41, H105 and D148, respectively
235 (Fig.5).
236
237 Predicted structures of the K56-2 and AU1054 TecA isoforms were determined by AlphaFold2
238 and displayed by PyMol (Fig.6). Results show that the overall folds and positions of catalytic
239 residues are highly similar (Fig.6). However, the presence of the non-conserved substitutions
240 R38G (charged to non-charged), G101T (non-polar to polar), and T146A (polar to non-polar) in
241 the vicinity of the active site (Fig.6) could impact the biological activity of the *B. orbicola* TecA
242 protein.
243
244
245 **Discussion**

246 The data presented above increase our understanding of the role of T6SS-1 and TecA in the
247 pathogenesis of *B. orbicola* and *B. cenocepacia* in the following three ways. First, our results
248 confirm that *B. cenocepacia* triggers inflammasome-dependent macrophage inflammatory death
249 by two mechanisms, one that is TecA and pyrin dependent and the other likely requires
250 detection of vacuole damage by caspase-11 (18). Second, *B. orbicola* via T6SS-1 triggers
251 TecA-dependent macrophage inflammatory death by two mechanisms, one that requires pyrin
252 and the other is inflammasome independent. Third, the TecA protein of *B. orbicola* appears to
253 comprise a separate subgroup of this effector superfamily, with distinct biological activity.
254 Together, these results indicate that the underlying mechanism of inflammation in chronic *B.*
255 *orbicola* and *B. cenocepacia* lung infections is multifactorial and species specific, which has
256 implications for treating this disease in pwCF.
257
258 J2315 and K56-2 are genomovar IIIA CF clinical isolates and members of the epidemic ET12
259 lineage common in Europe (39). Despite being clonal, the literature indicates that during
260 macrophage infections the T6SS-1 of J2315 is only detected by the pyrin inflammasome via
261 TecA (27, 32) while K56-2 is detected by the pyrin and caspase-11 inflammasomes (18, 25, 30).
262 Our results address this discrepancy by showing that when analyzed in parallel J2315 and K56-
263 2 both trigger pyrin-independent GSDMD cleavage in infected BMDMs. In addition, J2315
264 causes low but significant IL-1β release from *Mefv*$^{-/-}$ BMDMs under our infection conditions. It is
265 probable that caspase-11 is the proximal inflammasome activated in *Mefv*$^{-/-}$ BMDMs infected
266 with J2315 and K56-2. It will be important to carry out *B. cenocepacia* infection experiments with
267 BMDMs deficient in caspase-11 to confirm this hypothesis. Activation of caspase-11 by J2315
268 may not have been detected previously (27, 32) due to insufficient lengths of LPS priming of
269 *Mefv*$^{-/-}$ BMDMs. The two hour LPS priming used by Xu et al. and Aubert et al. (27, 32) may
270 have been insufficient to activate expression of caspase-11 (31). The overnight LPS priming we

271 use to activate expression of pyrin may have fortuitously allowed us to detect activation of
272 caspase-11 in *Mefv*$^{-/-}$ BMDMs infected with J2315 and K56-2.
273
274 Xu et al. found that lung inflammation in mice infected with J2315 required pyrin (27). However,
275 in preliminary experiments we observed only a subtle decrease in lung inflammation in mice
276 infected with J2315 (37). Experimental variables such as genetic or microbiota differences
277 between *Mefv*$^{-/-}$ mouse lines used by Xu et al. (27) and our study (37) could be responsible for
278 the discrepancy. However, our result can be explained by the data of Krause et al. (18) who
279 showed that caspase-11 is important for lung inflammation in mice infected with K56-2 (18).
280 Presumably, inflammation triggered by caspase-11 could partially compensate for the absence
281 of pyrin in *Mefv*$^{-/-}$ mice infected with J2315. It is possible that pyrin and caspase-11 contribute
282 additively to inflammation in lungs during *B. cenocepacia,* and this could be studied by directly
283 comparing responses to *B. cenocepacia* infection in mice that are *Mefv*$^{-/-}$ or *Casp11*$^{-/-}$ or
284 deficient in both inflammasomes. Interestingly, *Casp11*$^{-/-}$ mice had increased survival compared
285 to *Casp1*$^{+/+}$ mice, even though K56-2 growth was restricted better in the latter animals (18). This
286 result indicates that lethality in this context is due to immunopathology in the lung rather than
287 bacterial growth in per se.
288
289 The mechanism of caspase-11 activation by J2315 in macrophages is likely the same as K56-2,
290 where T6SS-1 has been shown to mediate phagosome damage (26). In fact, there is evidence
291 that J2315 escapes from damaged phagosomes (13, 14). The mechanism of phagosome
292 damage by *B. cenocepacia* T6SS-1 is unknown. Polymerized actin co-localizes with cytosolic
293 J2315 in human macrophages (13). However, the role of actin polymerization in phagosome
294 damage by *B. cenocepacia* is unclear. Additional evidence that *B. cenocepacia* escapes
295 phagosomes comes from the finding that J2315 activates non-inflammasome PRRs like
296 mitochondrial antiviral-signaling protein (MAVS) and stimulator of interferon genes (STING) in

297 macrophages (14). MAVS is activated primarily in response to viral RNAs, where STING is
298 activated in response to detection of bacterial double stranded DNA (dsDNA) (14). MAVS and
299 STING activation in macrophages leads to a type I interferon (IFN) response which induces
300 autophagy/xenophagy and was shown to counteract *B. cenocepacia* J2315 replication in
301 macrophages (14).
302
303 Our data suggest that *B. orbicola* TecA can trigger PMR in infected macrophages by an
304 inflammasome-independent mechanism because the lack of GSDMD cleavage in *Mefv*$^{-/-}$
305 macrophages indicates that caspase-1 and caspase-11 are not being activated. *B. orbicola*
306 TecA can trigger release of LDH from unprimed BMDMs (unpublished observation) further
307 suggesting this pathway of PMR is inflammasome independent. To confirm this concept, it will
308 be important to carry out *B. orbicola* infection experiments with BMDMs deficient in caspase-1
309 and -11. Release of HMGB1 could be measured to confirm that multiple DAMPs are being
310 released by PMR. It will also be important to determine if *B. orbicola* TecA triggers
311 inflammasome-independent PMR in human macrophages.
312
313 Recently the protein NINJ1 has been shown to be required for PMR downstream of multiple
314 forms of cell death in BMDMs (40). It is possible that NINJ1 is important for inflammasome-
315 independent PMR and release of DAMPs from *B. orbicola*-infected macrophages. Microscopy
316 could be used to confirm that inflammasome-independent DAMP release is associated with
317 plasma membrane damage in *Mefv*$^{-/-}$ macrophages infected with *B. orbicola*. Propidium iodide
318 uptake measured by fluorescence microscopy and cell rounding and blebbing as detected by
319 phase microscopy would be indicators of plasma membrane damage (41).
320
321 The existence of an inflammasome-independent PMR pathway in macrophages likely explains
322 why recruitment of inflammatory cells to lungs of mice infected with AU1054 is not decreased in

323 the absence of pyrin (37). We hypothesize *B. orbicola* TecA triggers redundant pathways of
324 macrophage inflammatory cell death both in vitro and in vivo. The pyrin-dependent pathway
325 results in IL-1β release and pyroptosis, while the inflammasome-independent pathway results in
326 PMR and release of multiple DAMPs. Either pathway can exacerbate inflammatory monocyte
327 recruitment and persistence in lungs infected with *B. orbicola* (37). For example, IL-1β or
328 DAMPs released from *B. orbicola*-infected alveolar macrophages could activate airway epithelial
329 cells to produce chemokines for inflammatory monocytes. Inflammatory monocytes use the
330 receptor CCR2 to migrate out of the bone marrow into sites of infection in response to the
331 chemokine CCL2 (42). Inflammatory monocytes can differentiate into macrophages and
332 depending on the context can cause detrimental immune responses in lung infections (42, 43).
333 Persistence of excessive numbers inflammatory monocyte-derived macrophages could cause
334 immunopathology in lungs infected with *B. orbicola* (37). Inflammatory monocyte-derived
335 macrophages recruited by CCL2 could also become infected with *B. orbicola* and release more
336 IL-1β or DAMPs, thus initiating a damaging cycle of inflammation.
337
338 Our finding that *B. orbicola* TecA triggers inflammasome-independent PMR suggests that the
339 10% amino acid variation in this isoform imparts different biological activity as compared to *B.*
340 *cenocepacia*. Although speculative we suggest that *B. orbicola* TecA deaminates a host protein
341 target which triggers PMR. To test the above hypothesis, it would be interesting to replace
342 TecA in AU1054 with the *B. cenocepacia* isoform and determine how this allele swap impacts
343 macrophage inflammatory death mechanisms upon bacterial infection.
344
345 **Acknowledgments**
346 We thank George O'Toole, John LiPuma, Feng Shao and Sergio Grinstein for providing
347 bacterial strains. Ericka A. Tamayo-Guevara helped produce the TecA AlphaFold structures

shown in Fig.6. This work was supported by grants from the Cystic Fibrosis Foundation (BLISKA22G0 and STANTO19R0) and support by DartCF through NIH grant P30-DK117469.

Materials and Methods

Bacterial strains: Bacterial strains used in this study are shown in Table 1. *B. orbicola* and *B. cenocepacia* strains were grown at 37°C on Luria-Bertani (LB) agar plates or in LB both with shaking.

Ethics statement: **I**solation of bone barrow cells from mice was carried out in accordance with a protocol that adhered to the Guide for the Care and Use of Laboratory Animals of the National Institutes of Health (NIH) and was reviewed and approved (approval #00002184) by the Institutional Animal Care and Use Committee at Dartmouth College. The Dartmouth College animal program is registered with the U.S. Department of Agriculture (USDA) through certificate number 12-R-0001, operates in accordance with Animal Welfare Assurance (NIH/PHS) under assurance number D16-00166 (A3259-01) and is accredited with the Association for Assessment and Accreditation of Laboratory Animal Care International (AAALAC, accreditation number 398).

Mouse strains: Wild-type (WT) C57BL/6J (stock# 000664) mice were purchased from Jackson Laboratories. Pyrin-knockout mice (*Mefv*$^{-/-}$) on the C57BL/6 background were obtained from Jae Chae and Daniel Kastner at the NIH (44) and bred in the mouse facilities at Dartmouth. Mice with the *Cftr*^{F508del} mutation on the C57BL/6 background were obtained from Case Western Reserve University's Cystic Fibrosis Mouse Models Core and bred at Dartmouth (37). *Mefv*$^{-/-}$ and *Cftr*^{F508del} mice were crossed to obtain breeding pairs that were *Cftr*^{F508del} *Mefv*$^{+/-}$ and *Cftr*^{F508del} *Mefv*$^{-/-}$. The resulting pups were genotyped as described (37) and used as a source of bone marrow cells.

Preparation of BMDMs: Bone marrow derived macrophages (BMDMs) were cultured from bone marrow of mice and cultured as described previously (37). After 7 days of differentiation the

374 BMDMs were seeded at a density of $0.8x10^6$ cells/well in 6-well plates in MGM 10/10 media
375 containing Dulbecco's Modified Eagle Medium (DMEM) + Glutamax (Gibco®) containing 10%
376 Fetal Bovine Serum (FBS) (GE®), 10% L929 cell-conditioned media, 1 mM sodium pyruvate
377 (Gibco®), 10 mM HEPES (Gibco®) and divided into 6-well plates at a density of $0.8 x10^6$
378 cells/well in a total volume of 3 mL. The BMDMs were primed with 100 ng/mL O26:B6
379 *Escherichia coli* LPS (Sigma®) and incubated overnight at 37°C with 5% CO_2.
380 BMDM infection assays: Overnight (16-hour) cultures of *B. orbicola* or *B. cenocepacia* were
381 subcultured 1:100 in fresh LB to OD_{600} = ~0.05 on infection day and shaken at 37°C until the
382 cultures reached mid-log phase (OD_{600} = 0.300). Cultures were then pelleted, the LB was
383 removed, and the bacteria were resuspended in PBS to the original volume (~$3x10^8$ CFU/mL).
384 The bacterial suspensions were then diluted to an MOI of 20 in warmed, in media lacking 10%
385 FBS (MGM 0/10). As a positive control for pyrin inflammasome activation, the
386 glucosyltransferase toxin from *Clostridium difficile* TcdB (List Biological Laboratories, Inc.) was
387 also diluted to 0.1mg/ml in warmed MGM 10. The BMDMs were washed once in warm 1x PBS
388 and 3ml fresh MGM 10 was added with bacteria or TcdB to the appropriate wells. The plates
389 were then centrifuged for 5 minutes at 1,000rpm to bring the bacteria and the cells in contact on
390 the bottom of the wells. The plates were incubated at 37°C with 5% CO_2 for 90 minutes. Cell
391 supernatants were collected for cytokine ELISAs and lactate dehydrogenase (LDH) assays. The
392 BMDMs were lysed using mammalian protein extraction reagent (M-PER, Thermo Scientific®)
393 with added cOmplete, Mini (Roche®) protease inhibitor and PhosSTOP (Roche®) phosphatase
394 inhibitor (37).
395 Western blotting: Five - 10mg of protein from the cell lysates were run on 4-12% NuPAGE Bis-
396 Tris SDS-PAGE gels (Invitrogen by ThermoFisher Scientific®) and transferred to PVDF
397 membranes (ThermoFisher Scientific®) using an iBlot 2 Gel Transfer Device (Life Technologies).
398 Membranes were blocked in 5% non-fat dairy milk and incubated with primary antibody
399 overnight. The primary antibodies used were rabbit MAb for GSDMD (Abcam®, ab209845), and

400 rabbit polyclonal for b-actin (Cell Signaling®, #4967). HRP-conjugated anti-rabbit (Jackson
401 laboratory) was used as a secondary antibody. Protein bands reacting with antibodies were
402 visualized using chemiluminescent detection reagent (GE Healthcare®) on an iBright FL1500
403 (ThermoFisher Scientific®).
404 IL-1β and IL-1α quantification: Murine IL-1β and IL-1α in BMDM supernatants was quantified
405 using ELISA kits (R&D Systems®, MLB00C and MLA00, DLB50, respectively) following the
406 manufacturer's instructions.
407 LDH quantification: LDH in BMDM supernatants was quantified using the CytoTox 96® Non-
408 Radioactive Cytotoxicity Assay (Promega®) following the manufacturer's instructions.
409 Statistical analysis of data: Experimental data generated from at least three independent in vitro
410 experiments are analyzed for significance. Probability (*p*) values for ELISA and LDH data are
411 calculated using one-way analysis of variance (ANOVA) or grouped two-way ANOVA with
412 Tukey's posttest.
413 TecA gene sequencing and protein sequence analysis: *B. orbicola* and *B. cenocepacia* were
414 grown on LB agar plates, single colonies were picked, suspended in sterile Elution Buffer
415 (Qiagen), and boiled for 5 minutes to release bacterial DNA. PCR was performed using the
416 colony DNA and primers that anneal upstream (Forward 5'-
417 ACGCCGTGACGGCCTGACGCCGT-3') and downstream (Reverse 5'-
418 GCGCGACGCCATGCGGAAATCGCCG-3') of all four *tecA* genes analyzed (BCAM1857 in
419 J2315, WQ49_RS04990 in K56-2, BCEN_RS18170 in AU1054 and EAY64595
420 in PC184). PCR products were run on a 1% agarose gel and purified using a Qiagen kit.
421 Purified DNA was sequenced and resulting sequences were analyzed, translated, and aligned
422 on SnapGene using ClustalW. Percent amino acid sequence identity was determined using
423 NCBI Protein BLAST. Predicted structures of the AU1054 and K56-2 TecA isoforms were
424 determined by AlphaFold2 (45) and displayed using PyMol.

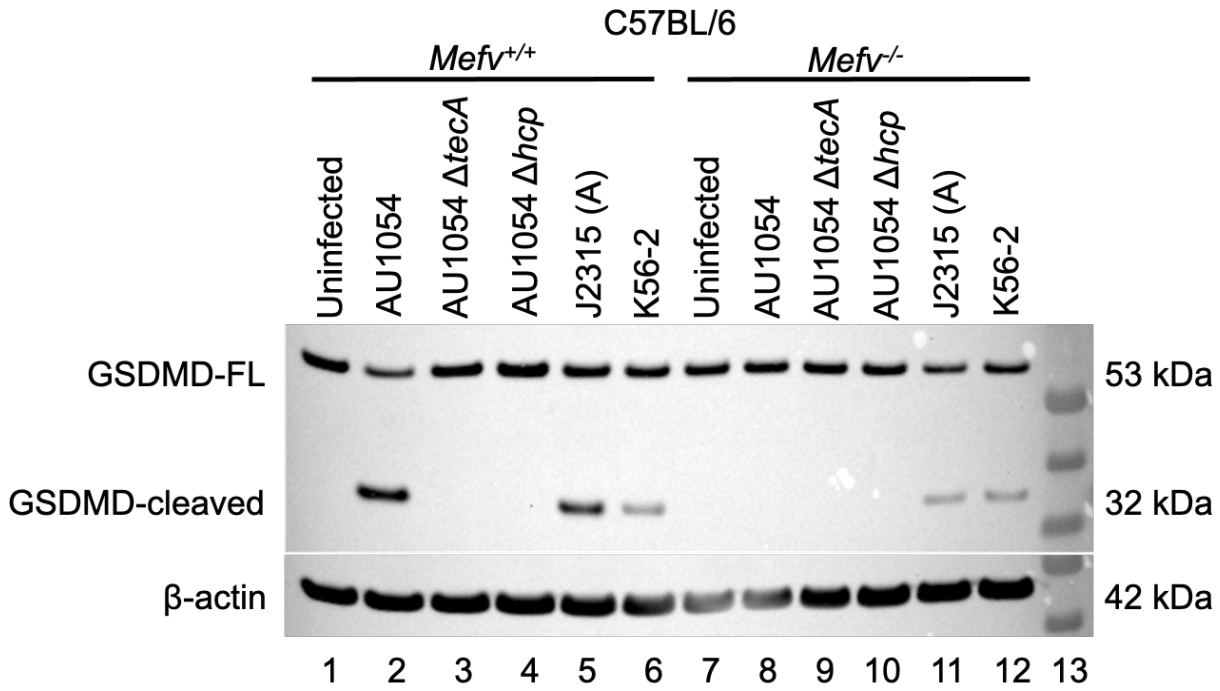

425

426 **Fig.1. Pyrin is differentially required for GSDMD cleavage in BMDMs infected with AU1054,**
427 **J2315 or K56-2**. LPS-primed C57BL/6 *Mefv*$^{+/+}$ or *Mefv*$^{-/-}$ BMDMs were left uninfected or infected
428 with the indicated strains (Table 1) for 90 min at MOI 20 and lysates were analyzed by
429 immunoblotting with antibodies to GSDMD or β-actin. Positions of GSDMD 53 kDa full length
430 (FL) and 32 kDa cleaved forms are indicated. Lane 13 is molecular weight (MW) ladder.

431

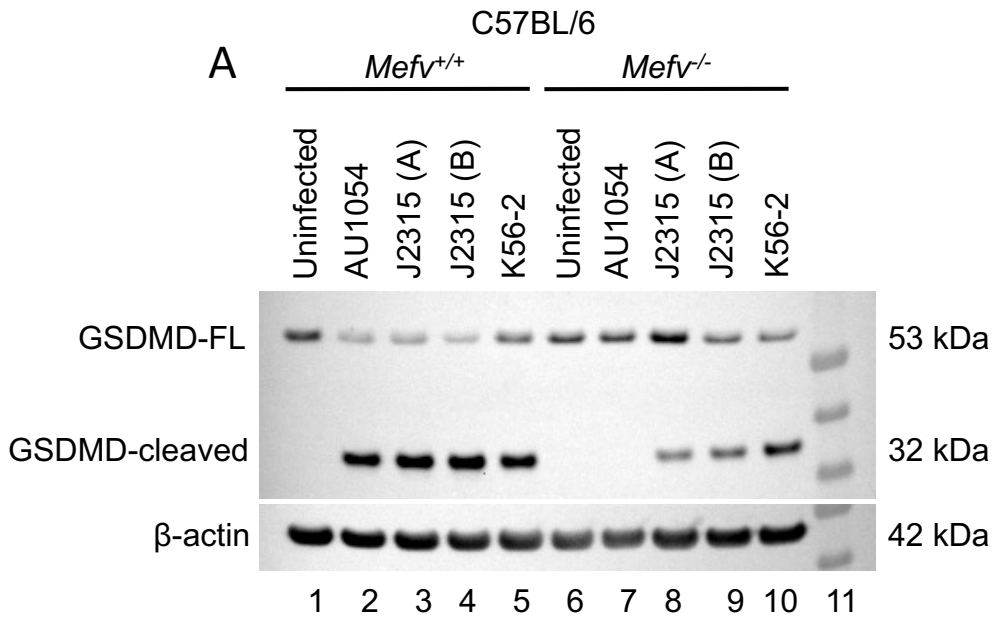

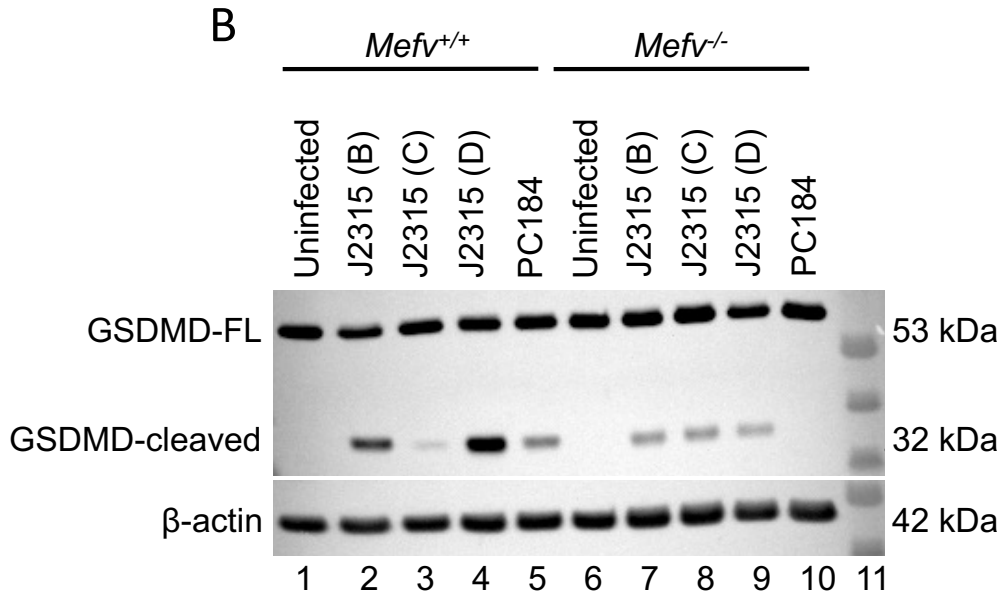

Fig.2. Pyrin is differentially required for GSDMD cleavage in BMDMs infected with *B. cenocepacia* and *B. orbicola*. LPS-primed C57BL/6 *Mefv*$^{+/+}$ and *Mefv*$^{-/-}$ BMDMs were left uninfected or infected for 90 min at MOI 20 with the indicated strains (Table 1) and lysates were analyzed by immunoblotting with antibodies to GSDMD or β-actin. The result in (B) with PC184 is representative of two independent experiments. Lanes 11 are a MW ladder.

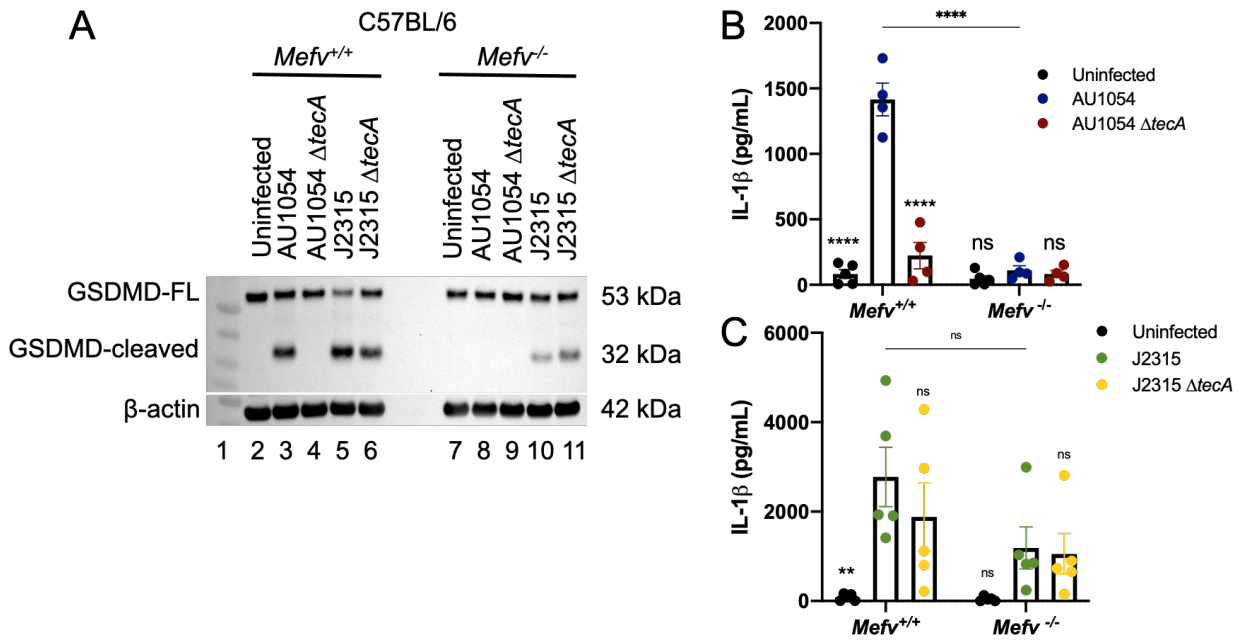

Fig.3. TecA is dispensable for pyrin-independent GSDMD cleavage and IL-1β release in BMDMs infected with J2315. LPS-primed C57BL/6 *Mefv*$^{+/+}$ or *Mefv*$^{-/-}$ BMDMs were left uninfected or infected with the indicated strains (Table 1) at an MOI of 20 for 90 minutes. (A) BMDM lysates were analyzed by immunoblotting with antibodies to GSDMD or β-actin. Lane 1 is a MW ladder. Cell supernatants were collected and analyzed for IL-1β by ELISA (B,C). Data shown in (B,C) are from four or five independent experiments, respectively. Error bars represent standard deviation. Significance determined by two-way ANOVA and Tukey posttest as compared to AU1054 (B) or J2315 (C) within and between BMDM genotypes. ns, not significant; * $p < 0.05$, ** $p < 0.01$, *** $p < 0.001$, **** $p < 0.0001$.

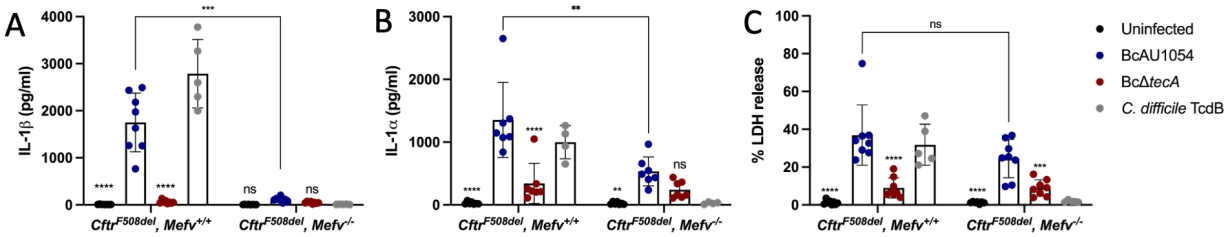

Fig.4. TecA triggers pyrin-independent IL-1α and LDH release from BMDMs infected with AU1054. LPS-primed *Cftr*^{F508del} *Mefv*$^{+/+}$ or *Mefv*$^{-/-}$ BMDMs were left uninfected or infected with AU1054 or AU1054 Δ*tecA* at an MOI of 20 or intoxicated with TcdB for 90 minutes. Cell supernatants were collected and analyzed for IL-1β (A) or IL-1α (B) by ELISA and PMR by LDH release (C). Data shown are from at least three independent experiments. Error bars represent standard deviation. Significance determined by two-way ANOVA as compared to AU1054 within and between BMDM genotypes. ns, not significant; ** $p < 0.01$, *** $p < 0.001$, **** $p < 0.0001$.

```
                10        20        30        40        50        60
TecA J2315      MQLTQLGGHVAQSGIAERQKHAQALMFGMANIDEYVSRGVCYDAAAYVRYLLRADALIAP  60
TecA K56-2      MQLTQLGGHVAQSGIAERQKHAQALMFGMANIDEYVSRGVCYDAAAYVRYLLRADALIAP  60
TecA AU1054     MQLTQLGGHVAQSGIAERQKHAQALMFGMANIDEYVSGGVCYDAAAYVRYLLRADAMIAP  60
TecA PC184      MQLTQLGGHVAQSGIAERQKHAQALMFGMSNIDEYVSGGVCYDAAAYVRYLLRADAMIAP  60

                70        80        90       100       110       120
TecA J2315      DALLDTAGQSWRTRFNFETGDQWDGRASIPAGTAVGFARGGNVFHAAIAVGGTRIRAING  120
TecA K56-2      DALLDTAGQSWRTRFNFETGDQWDGRASIPAGTAVGFARGGNVFHAAIAVGGTRIRAING  120
TecA AU1054     GTLLDTIGQLWKTRFNFETGNQWDGRASIPAGTAVGFARGTNVFHAAIAVGGTRIRGING  120
TecA PC184      GTLLDTIGQLWKTRFNFETGNQWDGRASIPAGTAVGFARGTNVFHAAIAVGGTRIRGING  120

                130       140       150
TecA J2315      GLLGAGWMNPVDLARALQPDPAGGFTYDRTTIRVHLSRL  159
TecA K56-2      GLLGAGWMNPVDLARALQPDPAGGFTYDRTTIRVHLSRL  159
TecA AU1054     GLLGAGWLHPVDLARVLQPDPAGGFAYDRTTIRVYLSRL  159
TecA PC184      GLLGAGWLHPVDLARVLQPDPAGGFAYDRTTIRVYLSRL  159
```

Fig.5. The TecA proteins of *B. cenocepacia* and *B. orbicola* exhibit amino acid variation. The *tecA* genes of the strains used in this study were sequenced and then translated and aligned in SnapGene using ClustalW. Amino acids highlighted in yellow indicate differences from the TecA sequence of J2315.

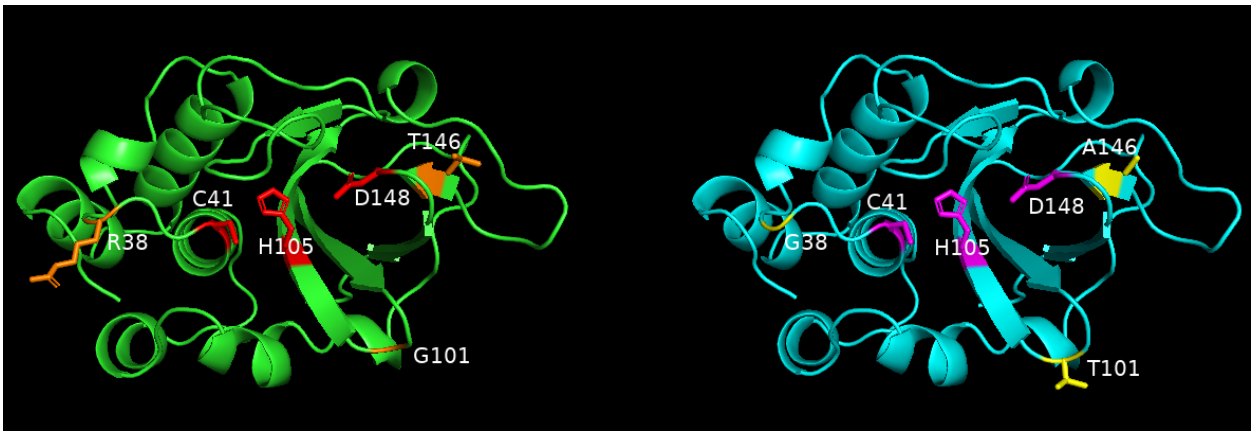

Fig.6. Comparison of predicted structures of TecA proteins of *B. cenocepacia* and *B. orbicola* and non-conserved amino acids adjacent to catalytic sites. Predicted structures of TecA proteins of K56-2 (left) and AU1054 (right) were generated using AlphaFold2 and displayed using PyMol. Catalytic residues are shown in red (left) or cyan (right). Non-conserved residues adjacent to catalytic sides are shown in orange (left) or yellow (right).

Species (Genomovar)	Lineage	Strain (Isolate)	Source, Collection, Reference
B. cenocepacia (Genomovar IIIA)	ET-12	J2315 (A)	Bliska strain collection, (37)
		J2315 (B)	George O'Toole
		J2315 (C; H12711)	John LiPuma, BCCM/LMG
		J2315 (D; H12718)	John LiPuma
		J2315 (E)	Feng Shao, BCCM/LMG, (32)
		J2315 Δ*tecA*	Feng Shao, (32)
		K56-2	George O'Toole
B. orbicola (Genomovar IIIB)	PHDC	AU1054	Peggy Cotter, (36)
		AU1054 Δ*hcp*	Peggy Cotter, (36)
		AU1054 Δ*tecA*	Peggy Cotter, (37)
	Midwest	PC184	John LiPuma, (46)

Table 1. *B. cenocepacia* and *B. orbicola* isolates used in this study. Letters in parentheses after J2315 are arbitrary identifiers for isolates used in this study. H12711 and H12718 are additional identifiers for these isolates obtained from John LiPuma. Belgian Coordinated Collections of Microorganisms (BCCM/LMG)

REFERENCES

1. Loutet SA, Valvano MA. A decade of Burkholderia cenocepacia virulence determinant research. Infect Immun. 2010;78(10):4088-100. doi: 10.1128/IAI.00212-10. PubMed PMID: 20643851; PMCID: PMC2950345.
2. Hauser AR, Jain M, Bar-Meir M, McColley SA. Clinical significance of microbial infection and adaptation in cystic fibrosis. Clin Microbiol Rev. 2011;24(1):29-70. Epub 2011/01/15. doi: 10.1128/CMR.00036-10. PubMed PMID: 21233507; PMCID: PMC3021203.
3. Scoffone VC, Chiarelli LR, Trespidi G, Mentasti M, Riccardi G, Buroni S. Burkholderia cenocepacia Infections in Cystic Fibrosis Patients: Drug Resistance and Therapeutic Approaches. Front Microbiol. 2017;8:1592. Epub 2017/09/08. doi: 10.3389/fmicb.2017.01592. PubMed PMID: 28878751; PMCID: PMC5572248.
4. De Soyza A, Meachery G, Hester KL, Nicholson A, Parry G, Tocewicz K, Pillay T, Clark S, Lordan JL, Schueler S, Fisher AJ, Dark JH, Gould FK, Corris PA. Lung transplantation for patients with cystic fibrosis and Burkholderia cepacia complex infection: a single-center experience. J Heart Lung Transplant. 2010;29(12):1395-404. Epub 2010/09/03. doi: 10.1016/j.healun.2010.06.007. PubMed PMID: 20810293.
5. Vandamme P, Holmes B, Coenye T, Goris J, Mahenthiralingam E, LiPuma JJ, Govan JR. Burkholderia cenocepacia sp. nov.--a new twist to an old story. Res Microbiol.

500 2003;154(2):91-6. Epub 2003/03/22. doi: 10.1016/S0923-2508(03)00026-3. PubMed PMID:
501 12648723.
502 6. Drevinek P, Mahenthiralingam E. Burkholderia cenocepacia in cystic fibrosis:
503 epidemiology and molecular mechanisms of virulence. Clin Microbiol Infect. 2010;16(7):821-30.
504 Epub 2010/10/01. doi: 10.1111/j.1469-0691.2010.03237.x. PubMed PMID: 20880411.
505 7. Ganesan S, Sajjan US. Host evasion by Burkholderia cenocepacia. Front Cell Infect
506 Microbiol. 2011;1:25. Epub 2011/01/01. doi: 10.3389/fcimb.2011.00025. PubMed PMID:
507 22919590; PMCID: PMC3417383.
508 8. Valvano MA. Intracellular survival of Burkholderia cepacia complex in phagocytic cells.
509 Can J Microbiol. 2015;61(9):607-15. doi: 10.1139/cjm-2015-0316. PubMed PMID: 26220706.
510 9. Abdulrahman BA, Khweek AA, Akhter A, Caution K, Kotrange S, Abdelaziz DH, Newland
511 C, Rosales-Reyes R, Kopp B, McCoy K, Montione R, Schlesinger LS, Gavrilin MA, Wewers MD,
512 Valvano MA, Amer AO. Autophagy stimulation by rapamycin suppresses lung inflammation and
513 infection by Burkholderia cenocepacia in a model of cystic fibrosis. Autophagy.
514 2011;7(11):1359-70. doi: 10.4161/auto.7.11.17660. PubMed PMID: 21997369; PMCID:
515 PMC3359483.
516 10. Assani K, Tazi MF, Amer AO, Kopp BT. IFN-gamma stimulates autophagy-mediated
517 clearance of Burkholderia cenocepacia in human cystic fibrosis macrophages. PLoS One.
518 2014;9(5):e96681. Epub 2014/05/07. doi: 10.1371/journal.pone.0096681. PubMed PMID:
519 24798083; PMCID: PMC4010498.
520 11. Schwab U, Abdullah LH, Perlmutt OS, Albert D, Davis CW, Arnold RR, Yankaskas JR,
521 Gilligan P, Neubauer H, Randell SH, Boucher RC. Localization of Burkholderia cepacia complex
522 bacteria in cystic fibrosis lungs and interactions with Pseudomonas aeruginosa in hypoxic
523 mucus. Infect Immun. 2014;82(11):4729-45. doi: 10.1128/IAI.01876-14. PubMed PMID:
524 25156735; PMCID: PMC4249344.
525 12. Sousa SA, Ulrich M, Bragonzi A, Burke M, Worlitzsch D, Leitao JH, Meisner C, Eberl L,
526 Sa-Correia I, Doring G. Virulence of Burkholderia cepacia complex strains in gp91phox-/- mice.
527 Cell Microbiol. 2007;9(12):2817-25. doi: 10.1111/j.1462-5822.2007.00998.x. PubMed PMID:
528 17627623.
529 13. Al-Khodor S, Marshall-Batty K, Nair V, Ding L, Greenberg DE, Fraser ID. Burkholderia
530 cenocepacia J2315 escapes to the cytosol and actively subverts autophagy in human
531 macrophages. Cell Microbiol. 2014;16(3):378-95. Epub 2013/10/15. doi: 10.1111/cmi.12223.
532 PubMed PMID: 24119232; PMCID: PMC3927784.
533 14. Dorrington MG, Bradfield CJ, Lack JB, Lin B, Liang JJ, Starr T, Ernst O, Gross JL, Sun
534 J, Miller AH, Steele-Mortimer O, Fraser IDC. Type I IFNs facilitate innate immune control of the
535 opportunistic bacteria Burkholderia cenocepacia in the macrophage cytosol. PLoS Pathog.
536 2021;17(3):e1009395. Epub 2021/03/09. doi: 10.1371/journal.ppat.1009395. PubMed PMID:
537 33684179; PMCID: PMC7971856.
538 15. Lamothe J, Huynh KK, Grinstein S, Valvano MA. Intracellular survival of Burkholderia
539 cenocepacia in macrophages is associated with a delay in the maturation of bacteria-containing
540 vacuoles. Cell Microbiol. 2007;9(1):40-53. Epub 2006/07/28. doi: 10.1111/j.1462-
541 5822.2006.00766.x. PubMed PMID: 16869828.
542 16. Keith KE, Hynes DW, Sholdice JE, Valvano MA. Delayed association of the NADPH
543 oxidase complex with macrophage vacuoles containing the opportunistic pathogen Burkholderia
544 cenocepacia. Microbiology (Reading). 2009;155(Pt 4):1004-15. Epub 2009/04/01. doi:
545 10.1099/mic.0.026781-0. PubMed PMID: 19332803.
546 17. Assani K, Shrestha CL, Robledo-Avila F, Rajaram MV, Partida-Sanchez S, Schlesinger
547 LS, Kopp BT. Human Cystic Fibrosis Macrophages Have Defective Calcium-Dependent Protein
548 Kinase C Activation of the NADPH Oxidase, an Effect Augmented by Burkholderia cenocepacia.
549 J Immunol. 2017;198(5):1985-94. Epub 2017/01/18. doi: 10.4049/jimmunol.1502609. PubMed
550 PMID: 28093527; PMCID: PMC5322234.

551 18. Krause K, Caution K, Badr A, Hamilton K, Saleh A, Patel K, Seveau S, Hall-Stoodley L,
552 Hegazi R, Zhang X, Gavrilin MA, Amer AO. CASP4/caspase-11 promotes autophagosome
553 formation in response to bacterial infection. Autophagy. 2018;14(11):1928-42. Epub 2018/09/01.
554 doi: 10.1080/15548627.2018.1491494. PubMed PMID: 30165781; PMCID: PMC6152495.
555 19. Hunt TA, Kooi C, Sokol PA, Valvano MA. Identification of Burkholderia cenocepacia
556 genes required for bacterial survival in vivo. Infect Immun. 2004;72(7):4010-22. Epub
557 2004/06/24. doi: 10.1128/IAI.72.7.4010-4022.2004. PubMed PMID: 15213146; PMCID:
558 PMC427415.
559 20. Wood TE, Howard SA, Wettstadt S, Filloux A. PAAR proteins act as the 'sorting hat' of
560 the type VI secretion system. Microbiology (Reading). 2019;165(11):1203-18. Epub 2019/08/06.
561 doi: 10.1099/mic.0.000842. PubMed PMID: 31380737; PMCID: PMC7376260.
562 21. Hachani A, Wood TE, Filloux A. Type VI secretion and anti-host effectors. Curr Opin
563 Microbiol. 2016;29:81-93. Epub 2016/01/02. doi: 10.1016/j.mib.2015.11.006. PubMed PMID:
564 26722980.
565 22. Spiewak HL, Shastri S, Zhang L, Schwager S, Eberl L, Vergunst AC, Thomas MS.
566 Burkholderia cenocepacia utilizes a type VI secretion system for bacterial competition.
567 Microbiologyopen. 2019:e774. Epub 2019/01/11. doi: 10.1002/mbo3.774. PubMed PMID:
568 30628184; PMCID: PMC6612558.
569 23. Flannagan RS, Jaumouille V, Huynh KK, Plumb JD, Downey GP, Valvano MA, Grinstein
570 S. Burkholderia cenocepacia disrupts host cell actin cytoskeleton by inactivating Rac and
571 Cdc42. Cell Microbiol. 2012;14(2):239-54. Epub 2011/10/26. doi: 10.1111/j.1462-
572 5822.2011.01715.x. PubMed PMID: 22023324.
573 24. Rosales-Reyes R, Skeldon AM, Aubert DF, Valvano MA. The Type VI secretion system
574 of Burkholderia cenocepacia affects multiple Rho family GTPases disrupting the actin
575 cytoskeleton and the assembly of NADPH oxidase complex in macrophages. Cell Microbiol.
576 2012;14(2):255-73. Epub 2011/10/26. doi: 10.1111/j.1462-5822.2011.01716.x. PubMed PMID:
577 22023353.
578 25. Gavrilin MA, Abdelaziz DH, Mostafa M, Abdulrahman BA, Grandhi J, Akhter A, Abu
579 Khweek A, Aubert DF, Valvano MA, Wewers MD, Amer AO. Activation of the pyrin
580 inflammasome by intracellular Burkholderia cenocepacia. J Immunol. 2012;188(7):3469-77. doi:
581 10.4049/jimmunol.1102272. PubMed PMID: 22368275; PMCID: PMC3482472.
582 26. Rosales-Reyes R, Aubert DF, Tolman JS, Amer AO, Valvano MA. Burkholderia
583 cenocepacia type VI secretion system mediates escape of type II secreted proteins into the
584 cytoplasm of infected macrophages. PLoS One. 2012;7(7):e41726. Epub 2012/08/01. doi:
585 10.1371/journal.pone.0041726. PubMed PMID: 22848580; PMCID: PMC3405007.
586 27. Xu H, Yang J, Gao W, Li L, Li P, Zhang L, Gong YN, Peng X, Xi JJ, Chen S, Wang F,
587 Shao F. Innate immune sensing of bacterial modifications of Rho GTPases by the Pyrin
588 inflammasome. Nature. 2014;513(7517):237-41. doi: 10.1038/nature13449. PubMed PMID:
589 24919149.
590 28. Zhao Y, Shao F. Diverse mechanisms for inflammasome sensing of cytosolic bacteria
591 and bacterial virulence. Curr Opin Microbiol. 2016;29:37-42. Epub 2015/11/13. doi:
592 10.1016/j.mib.2015.10.003. PubMed PMID: 26562791.
593 29. Shi J, Gao W, Shao F. Pyroptosis: Gasdermin-Mediated Programmed Necrotic Cell
594 Death. Trends Biochem Sci. 2017;42(4):245-54. doi: 10.1016/j.tibs.2016.10.004. PubMed PMID:
595 27932073.
596 30. Estfanous S, Krause K, Anne MNK, Eltobgy M, Caution K, Abu Khweek A, Hamilton K,
597 Badr A, Daily K, Carafice C, Baetzhold D, Zhang X, Li T, Wen H, Gavrilin MA, Haffez H, Soror
598 S, Amer AO. Gasdermin D restricts Burkholderia cenocepacia infection in vitro and in vivo. Sci
599 Rep. 2021;11(1):855. Epub 2021/01/15. doi: 10.1038/s41598-020-79201-5. PubMed PMID:
600 33441602; PMCID: PMC7807041.

601 31. Broz P, Monack DM. Noncanonical inflammasomes: caspase-11 activation and effector
602 mechanisms. PLoS Pathog. 2013;9(2):e1003144. Epub 2013/03/08. doi:
603 10.1371/journal.ppat.1003144
604 PPATHOGENS-D-12-02639 [pii]. PubMed PMID: 23468620; PMCID: 3585133.
605 32. Aubert DF, Xu H, Yang J, Shi X, Gao W, Li L, Bisaro F, Chen S, Valvano MA, Shao F. A
606 Burkholderia Type VI Effector Deamidates Rho GTPases to Activate the Pyrin Inflammasome
607 and Trigger Inflammation. Cell Host Microbe. 2016;19(5):664-74. doi:
608 10.1016/j.chom.2016.04.004. PubMed PMID: 27133449.
609 33. Walpole GFW, Plumb JD, Chung D, Tang B, Boulay B, Osborne DG, Piotrowski JT, Catz
610 SD, Billadeau DD, Grinstein S, Jaumouille V. Inactivation of Rho GTPases by Burkholderia
611 cenocepacia Induces a WASH-Mediated Actin Polymerization that Delays Phagosome
612 Maturation. Cell Rep. 2020;31(9):107721. Epub 2020/06/04. doi: 10.1016/j.celrep.2020.107721.
613 PubMed PMID: 32492429; PMCID: PMC7315377.
614 34. Wallner A, King E, Ngonkeu ELM, Moulin L, Bena G. Genomic analyses of Burkholderia
615 cenocepacia reveal multiple species with differential host-adaptation to plants and humans.
616 BMC Genomics. 2019;20(1):803. Epub 2019/11/07. doi: 10.1186/s12864-019-6186-z. PubMed
617 PMID: 31684866; PMCID: PMC6829993.
618 35. Morales-Ruiz LM, Rodriguez-Cisneros M, Kerber-Diaz JC, Rojas-Rojas FU, Ibarra JA,
619 Estrada-de Los Santos P. Burkholderia orbicola sp. nov., a novel species within the
620 Burkholderia cepacia complex. Arch Microbiol. 2022;204(3):178. Epub 2022/02/18. doi:
621 10.1007/s00203-022-02778-0. PubMed PMID: 35174425.
622 36. Perault AI, Chandler CE, Rasko DA, Ernst RK, Wolfgang MC, Cotter PA. Host
623 Adaptation Predisposes Pseudomonas aeruginosa to Type VI Secretion System-Mediated
624 Predation by the Burkholderia cepacia Complex. Cell Host Microbe. 2020;28(4):534-47 e3.
625 Epub 2020/08/07. doi: 10.1016/j.chom.2020.06.019. PubMed PMID: 32755549; PMCID:
626 PMC7554260.
627 37. Loeven NA, Perault AI, Cotter PA, Hodges CA, Schwartzman JD, Hampton TH, Bliska
628 JB. The Burkholderia cenocepacia Type VI Secretion System Effector TecA Is a Virulence
629 Factor in Mouse Models of Lung Infection. mBio. 2021;12(5):e0209821. Epub 2021/09/29. doi:
630 10.1128/mBio.02098-21. PubMed PMID: 34579569; PMCID: PMC8546862.
631 38. Di Paolo NC, Shayakhmetov DM. Interleukin 1alpha and the inflammatory process. Nat
632 Immunol. 2016;17(8):906-13. Epub 2016/07/21. doi: 10.1038/ni.3503. PubMed PMID:
633 27434011; PMCID: PMC5152572.
634 39. Holden MT, Seth-Smith HM, Crossman LC, Sebaihia M, Bentley SD, Cerdeno-Tarraga
635 AM, Thomson NR, Bason N, Quail MA, Sharp S, Cherevach I, Churcher C, Goodhead I, Hauser
636 H, Holroyd N, Mungall K, Scott P, Walker D, White B, Rose H, Iversen P, Mil-Homens D, Rocha
637 EP, Fialho AM, Baldwin A, Dowson C, Barrell BG, Govan JR, Vandamme P, Hart CA,
638 Mahenthiralingam E, Parkhill J. The genome of Burkholderia cenocepacia J2315, an epidemic
639 pathogen of cystic fibrosis patients. J Bacteriol. 2009;191(1):261-77. Epub 2008/10/22. doi:
640 10.1128/JB.01230-08. PubMed PMID: 18931103; PMCID: PMC2612433.
641 40. Kayagaki N, Kornfeld OS, Lee BL, Stowe IB, O'Rourke K, Li Q, Sandoval W, Yan D,
642 Kang J, Xu M, Zhang J, Lee WP, McKenzie BS, Ulas G, Payandeh J, Roose-Girma M,
643 Modrusan Z, Reja R, Sagolla M, Webster JD, Cho V, Andrews TD, Morris LX, Miosge LA,
644 Goodnow CC, Bertram EM, Dixit VM. NINJ1 mediates plasma membrane rupture during lytic
645 cell death. Nature. 2021;591(7848):131-6. Epub 2021/01/21. doi: 10.1038/s41586-021-03218-7.
646 PubMed PMID: 33472215.
647 41. Fink SL, Cookson BT. Apoptosis, pyroptosis, and necrosis: mechanistic description of
648 dead and dying eukaryotic cells. Infect Immun. 2005;73(4):1907-16. Epub 2005/03/24. doi:
649 73/4/1907 [pii]
650 10.1128/IAI.73.4.1907-1916.2005. PubMed PMID: 15784530; PMCID: 1087413.

651 42. Serbina NV, Jia T, Hohl TM, Pamer EG. Monocyte-mediated defense against microbial
652 pathogens. Annu Rev Immunol. 2008;26:421-52. Epub 2008/02/29. doi:
653 10.1146/annurev.immunol.26.021607.090326. PubMed PMID: 18303997.
654 43. Heung LJ, Hohl TM. Inflammatory monocytes are detrimental to the host immune
655 response during acute infection with Cryptococcus neoformans. PLoS Pathog.
656 2019;15(3):e1007627. Epub 2019/03/22. doi: 10.1371/journal.ppat.1007627. PubMed PMID:
657 30897162; PMCID: PMC6428256.
658 44. Chae JJ, Cho YH, Lee GS, Cheng J, Liu PP, Feigenbaum L, Katz SI, Kastner DL. Gain-
659 of-function Pyrin mutations induce NLRP3 protein-independent interleukin-1beta activation and
660 severe autoinflammation in mice. Immunity. 2011;34(5):755-68. doi:
661 10.1016/j.immuni.2011.02.020. PubMed PMID: 21600797; PMCID: PMC3129608.
662 45. Jumper J, Evans R, Pritzel A, Green T, Figurnov M, Ronneberger O, Tunyasuvunakool
663 K, Bates R, Zidek A, Potapenko A, Bridgland A, Meyer C, Kohl SAA, Ballard AJ, Cowie A,
664 Romera-Paredes B, Nikolov S, Jain R, Adler J, Back T, Petersen S, Reiman D, Clancy E,
665 Zielinski M, Steinegger M, Pacholska M, Berghammer T, Bodenstein S, Silver D, Vinyals O,
666 Senior AW, Kavukcuoglu K, Kohli P, Hassabis D. Highly accurate protein structure prediction
667 with AlphaFold. Nature. 2021;596(7873):583-9. Epub 2021/07/16. doi: 10.1038/s41586-021-
668 03819-2. PubMed PMID: 34265844; PMCID: PMC8371605 have filed non-provisional patent
669 applications 16/701,070 and PCT/EP2020/084238, and provisional patent applications
670 63/107,362, 63/118,917, 63/118,918, 63/118,921 and 63/118,919, each in the name of
671 DeepMind Technologies Limited, each pending, relating to machine learning for predicting
672 protein structures. The other authors declare no competing interests.
673 46. Kim JY, Sajjan US, Krasan GP, LiPuma JJ. Disruption of tight junctions during traversal
674 of the respiratory epithelium by Burkholderia cenocepacia. Infect Immun. 2005;73(11):7107-12.
675 Epub 2005/10/22. doi: 10.1128/IAI.73.11.7107-7112.2005. PubMed PMID: 16239504; PMCID:
676 PMC1273860.
677